



UvA-DARE (Digital Academic Repository)

Thermal expansion and magnetostriction of superconduct URu₂Si₂

van Dijk, N.H.; de Visser, A.; Franse, J.J.M.; Menovsky, A.A.

Publication date
1995

Published in
Physical Review. B, Condensed Matter

[Link to publication](#)

Citation for published version (APA):

van Dijk, N. H., de Visser, A., Franse, J. J. M., & Menovsky, A. A. (1995). Thermal expansion and magnetostriction of superconduct URu₂Si₂. *Physical Review. B, Condensed Matter*, 51, 12665-12672.

General rights

It is not permitted to download or to forward/distribute the text or part of it without the consent of the author(s) and/or copyright holder(s), other than for strictly personal, individual use, unless the work is under an open content license (like Creative Commons).

Disclaimer/Complaints regulations

If you believe that digital publication of certain material infringes any of your rights or (privacy) interests, please let the Library know, stating your reasons. In case of a legitimate complaint, the Library will make the material inaccessible and/or remove it from the website. Please Ask the Library: <https://uba.uva.nl/en/contact>, or a letter to: Library of the University of Amsterdam, Secretariat, Singel 425, 1012 WP Amsterdam, The Netherlands. You will be contacted as soon as possible.

Thermal expansion and magnetostriction of superconducting URu₂Si₂

N. H. van Dijk, A. de Visser, J. J. M. Franse, and A. A. Menovsky

Van der Waals-Zeeman Laboratory, University of Amsterdam, Valckenierstraat 65, 1018 XE Amsterdam, The Netherlands

(Received 11 October 1994)

Dilatation measurements have been performed on a single-crystalline sample of the heavy-fermion superconductor URu₂Si₂ ($T_c = 1.2$ K). Thermal-expansion measurements in combination with specific-heat data reveal a thermal electronic Grüneisen parameter of $\Gamma_T = 27$. A comparison with the magnetic electronic Grüneisen parameter derived from the magnetostriction, $\Gamma_B = 26$, points to a single energy scale. The measured magnetostriction is strongly anisotropic with a peculiar hysteresis. Close to the upper critical field, a change of sign in the magnetostrictive hysteresis is observed.

I. INTRODUCTION

Among the intermetallic compounds with the tetragonal ThCr₂Si₂ structure, URu₂Si₂ attracts considerable attention because of the unusual coexistence of superconductivity and antiferromagnetism.¹⁻⁴ Long-range antiferromagnetic order is found below the Néel temperature $T_N = 17.5$ K. The pronounced anomalies in the specific heat and electrical resistivity at T_N (Refs. 1-4) reveal that the antiferromagnetic order is of the spin-density-wave type with a gap ($\Delta \sim 130$ K) opening up over a part of the Fermi surface. For $T < T_N$ pronounced electronic interactions persist, which give rise to an enhanced value of the coefficient of the linear electronic term in the specific heat: $\gamma = 65$ mJ/mol K². Because of this enhanced γ value, URu₂Si₂ is classified as a heavy-fermion compound with a quasiparticle mass of the order of 50 times the free-electron mass. Neutron-diffraction experiments^{5,6} revealed that URu₂Si₂ is a type-I antiferromagnet with an extremely small ordered moment of $(0.03 \pm 0.01)\mu_B$ (on the uranium atom) oriented along the tetragonal axis (c axis). Assuming the uranium atoms to be tetravalent (³H₄ configuration), the magnetic properties can be explained to a certain extent by a crystal-field model with singlet-singlet-induced magnetic ordering (with an energy separation between the ground-state singlet and first excited singlet of 42 K).⁷ However, theory has failed so far to account for the unusually small ordered moment and therefore its origin is still the subject of lively debates. Reduced-moment antiferromagnetism appears to be a general feature of heavy-fermion compounds, and is more generally ascribed to strong c - f hybridization.

Surprisingly, superconductivity is found below $T_c = 1.2$ K.¹⁻⁴ The fairly large jump in the specific heat at T_c ($\Delta c / \gamma T_c \approx 0.8$) evidences heavy-fermion superconductivity, as the heavy quasiparticles form the superconducting condensate. Neutron-diffraction experiments have revealed that superconductivity and antiferromagnetic order coexist.⁵ The superconducting properties deviate strongly from the standard BCS behavior. The upper critical field B_{c2} is strongly anisotropic and unusually large: $B_{c2}(T \rightarrow 0)$ amounts to 14 T for $B \parallel c$ and to 3 T for

$B \parallel c$.⁸ The specific heat in the superconducting state is proportional to T^2 ,⁹ while the NMR spin-lattice relaxation rate T_1^{-1} varies approximately as T^3 .¹⁰ The power-law temperature dependence of the electronic excitation spectrum indicates an anisotropic gap structure (with nodes in the gap), which is in general attributed to unconventional superconductivity ($L \neq 0$). Recently, point-contact spectroscopy data¹¹ were taken as evidence that URu₂Si₂ has a line of nodes in the superconducting gap.

In this paper we report on an investigation of the unusual superconducting properties of a high-quality single-crystalline sample of URu₂Si₂ by means of a detailed dilatometry study (thermal expansion and magnetostriction) carried out in the temperature range $0.3 < T < 1.5$ K and magnetic-field range up to 5 T. The results enable us to calculate the (uniaxial) pressure dependence of the parameters characterizing the superconducting state. Furthermore, a peculiar hysteresis is found in the magnetostriction in the superconducting state, which is attributed to flux-pinning effects.

Earlier dilatometry experiments,⁴ performed in the normal state ($1.4 < T < 100$ K) on a monocrystalline sample, revealed a strong anisotropy in the linear coefficients of thermal expansion, α_{\parallel} and α_{\perp} [where \parallel and \perp refer to dilatation (contraction) along or perpendicular to the tetragonal axis]. Large jumps of opposite sign in α_{\parallel} and α_{\perp} at T_N signal the antiferromagnetic transition. At low temperatures, the data yielded a heavy-fermion Grüneisen parameter of $\Gamma = -d \ln T^* / d \ln V = 25$ (here T^* is the energy scale of the heavy-fermion resonance). Subsequent experiments¹² down to $T = 0.3$ K on the same sample revealed a rather broad superconducting transition accompanied by an inversion of the anisotropy in α_{\parallel} and α_{\perp} . The normal-state magnetostriction¹³ measured at $T = 4.2$ and 20 K for $B < 8$ T showed strongly anisotropic paramagnetic behavior ($\Delta L / L \propto B^2$). For $B \parallel c$, $\Delta V / V$ is almost two orders of magnitude larger than for $B \parallel a$.

The paper is organized as follows. After a description of the experimental setup, the results of the thermal expansion and magnetostriction experiments are presented. Subsequently, the normal-state electronic and magnetic properties of URu₂Si₂ are analyzed in terms of Grüneisen parameters. Next, the thermodynamic properties at the

superconducting transition are studied in terms of the Ehrenfest relations. Finally, the magnetostriction in the superconducting state is discussed, with special attention devoted to the magnetostrictive hysteresis.

II. EXPERIMENT

A single-crystalline batch of URu_2Si_2 was grown in a triarc furnace under a continuously titanium-gettered argon atmosphere by the Czochralski method.¹⁴ The single crystal was subsequently annealed for 7 days at 950°C. By means of spark erosion a rectangular barlike sample was cut along the principal crystallographic directions. The dimensions of the sample amount to $4 \times 3 \times 5 \text{ mm}^3$ ($a \times a \times c$). Dilatation measurements were carried out using a sensitive three-terminal parallel-plate capacitance technique. The dilatation cell, machined of oxygen-free high-conductivity copper,¹⁵ was attached to the cold plate of a ^3He cryostat, which was operated by an adsorption pump. Temperatures were read with a RuO_2 chip resistor that was in good thermal contact with the cold plate. The RuO_2 thermometer was calibrated in magnetic field using a field-insensitive capacitance thermometer.

The thermal-expansion measurements (in a field $\mathbf{B} \parallel c$) were performed for a dilatation (contraction) along the a and the c axis of the tetragonal crystal structure. The coefficient of linear thermal expansion, $\alpha_i = L^{-1} dL/dT$, where i refers to the a or the c axis, was measured stepwise ($\Delta T \approx 40 \text{ mK}$), in order to ensure thermal equilibrium of sample, cell, and thermometer during the measurement. The data have been corrected for the cell effect, i.e., the signal of the cell with a dummy copper sample. The linear magnetostriction, $\lambda = [L(B) - L(0)]/L(0)$, was measured for $\mathbf{B} \parallel a$ and $\mathbf{B} \parallel c$. For both field orientations λ was measured for a dilatation (contraction) direction along and perpendicular to the magnetic field. The magnetostriction was measured by recording the capacitance change while sweeping the magnetic field at a low rate ($dB/dt \leq 0.1 \text{ T/min}$). The coefficient of linear magnetostriction $\tau = d\lambda/dB$ can be determined by differentiating numerically the $\lambda(B)$ curves. Complementary λ versus B data were taken by a discrete method, i.e., by stepwise increasing the magnetic field ($\Delta B = 0.2 \text{ T}$) at fixed temperature. The accuracy of the data is determined by an error of 3% in the absolute value of $\Delta L/L$ due to the uncertainty in the effective area of the capacitance plates and a maximum sensitivity of 2×10^{-10} .

III. RESULTS

A. Thermal expansion

The temperature variation of α_a and α_c of URu_2Si_2 at low temperatures is shown in Fig. 1. The corresponding coefficient of volume expansion $\alpha_v = 2\alpha_a + \alpha_c$ is given by the solid line. For $T_c < T < 2 \text{ K}$, α_a , α_c , and α_v vary linearly with temperature as does the specific heat ($c = \gamma T$). The linear coefficients of the thermal expansion amount to $a_a = \alpha_a/T = 0.22 \times 10^{-6} \text{ K}^{-2}$ and $a_c = \alpha_c/T = -0.16 \times 10^{-6} \text{ K}^{-2}$. At the superconducting transition ($T_c = 1.18 \text{ K}$) α_a and α_c exhibit sharp jumps and change sign. The width of the superconducting tran-

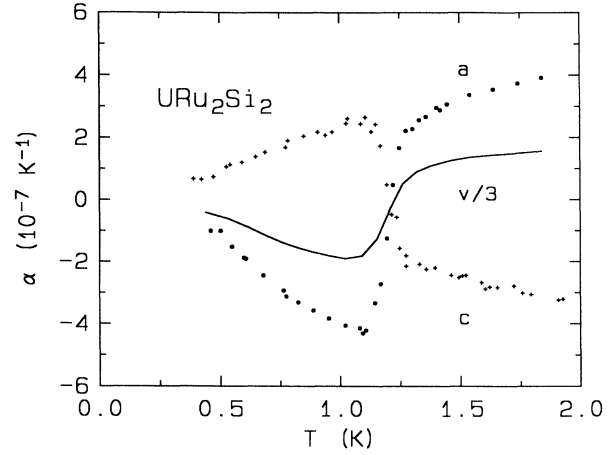


FIG. 1. Linear thermal expansion α_a (●) and α_c (+). The volume effect divided by 3 is indicated by the solid line.

sition amounts to 130 mK. The results displayed in Fig. 1 are in good agreement with previous measurements on a single-crystalline sample,¹² which exhibited a much broader transition ($\Delta T_c = 0.3 \text{ K}$). Thermal-expansion data in applied magnetic fields ($\mathbf{B} \parallel c$) are shown in Figs. 2 and 3. Superconductivity is progressively suppressed, initially at a rate $dT_c/dB = -0.16 \text{ K/T}$. The normal-state thermal expansion also shows a substantial reduction for $\mathbf{B} \parallel c$.

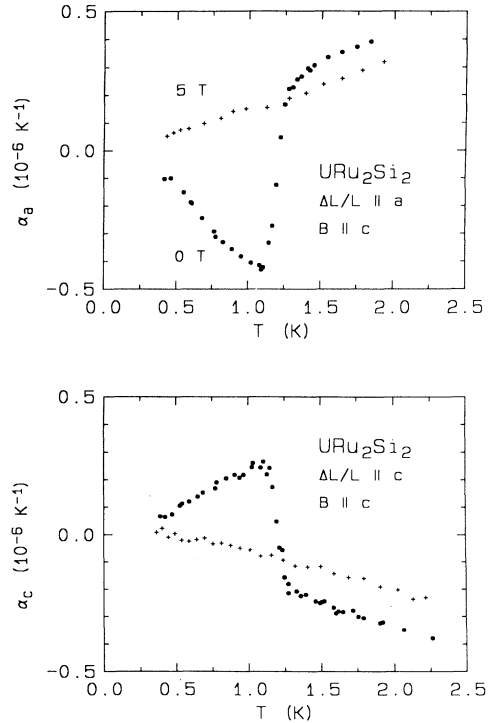


FIG. 2. Coefficients of linear thermal expansion α_a and α_c of URu_2Si_2 in zero field (●) and in a field of 5 T (+) oriented along the c axis. The jumps in α_a and α_c indicate the superconducting transition at $T_c = 1.18 \text{ K}$.

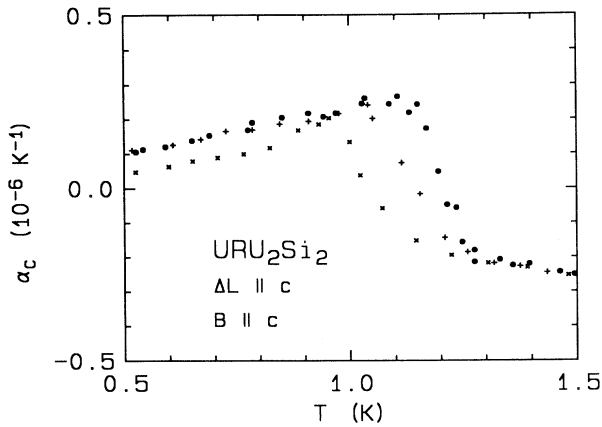


FIG. 3. Linear thermal expansion along the c axis in zero field (\bullet), in a field of 0.5 T ($+$), and in 1.0 T (\times) for $\mathbf{B}\parallel c$. The superconducting transition temperature is suppressed at a rate of $dT_c/dB = -0.16$ K/T.

B. Specific heat

The specific-heat data round T_c , as measured on an adjacent piece cut from the same annealed single-crystalline batch, are shown in Fig. 4. The normal-state γ value amounts to 67 mJ/mol K². In the superconducting state, a T^2 temperature dependence is found down to 350 mK. Extrapolation of the T^2 law down to 0 K indicates a vanishing γ value. The power-law temperature dependence is characteristic for unconventional superconductivity with a line of nodes in the superconducting gap.¹⁶ Using an equal-entropy construction a T_c value of 1.18 K is found, in good agreement with the thermal-expansion results. The relative jump in the specific heat at T_c amounts to $\Delta c/\gamma T_c = 0.81$, which is considerably smaller than the BCS value of 1.43, as expected for a strongly anisotropic superconducting gap. The specific-heat data reveal that our URu₂Si₂ sample is of a relatively high quality. Similar specific-heat data on samples of comparable

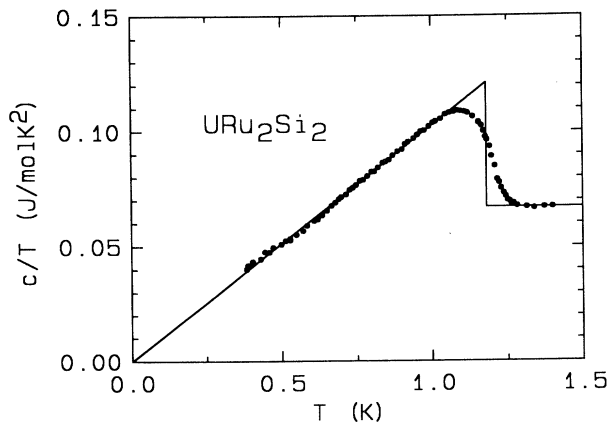


FIG. 4. Specific heat of URu₂Si₂ with a superconducting transition at $T_c = 1.18$ K. The solid line indicates a fit according to an equal-entropy construction. A T^2 temperature dependence of the specific heat is found in the superconducting state.

quality have recently been reported by Knetsch *et al.*¹⁷ and Brison *et al.*⁸

C. Magnetostriction

The curves of linear magnetostriction for fields up to 5 T ($\mathbf{B}\parallel a$ and $\mathbf{B}\parallel c$) measured in the normal state at $T = 1.5$ K are shown in Fig. 5. Data have been obtained for a dilatation (contraction) along the a (λ_a), b (λ_b), and c (λ_c) axis (here the b axis is defined as orthogonal to the a and c axes). The linear magnetization is highly anisotropic with a relatively strong field effect along the easy axis for magnetization ($\mathbf{B}\parallel c$) and a weak field effect along the hard magnetic axis ($\mathbf{B}\parallel a$). No hysteresis was observed. The volume magnetostriction is given by $\lambda_v = \lambda_a + \lambda_b + \lambda_c$ (note that symmetry arguments imply $\lambda_a = \lambda_b$ for $\mathbf{B}\parallel c$). The magnetostriction in the normal state behaves like $\lambda = bB^2$, characteristic for paramagnetic systems. The measured coefficients b are listed in Table I. Previous magnetostriction data¹³ in fields ($\mathbf{B}\parallel c$) up to 8 T at temperatures of 4.2 and 20 K yielded a similar behavior. The reported coefficients are $b_a = 6.0 \times 10^{-8}$ T⁻² and $b_c = -3.6 \times 10^{-8}$ T⁻² at 4.2 K, values which are close to the data listed in Table I.

The linear magnetostriction in the superconducting state was measured with a sweep method as well as with a discrete method. The experimental results for λ_c and $\mathbf{B}\parallel c$ obtained by the sweep method are shown in Fig. 6 for several temperatures. In the superconducting state

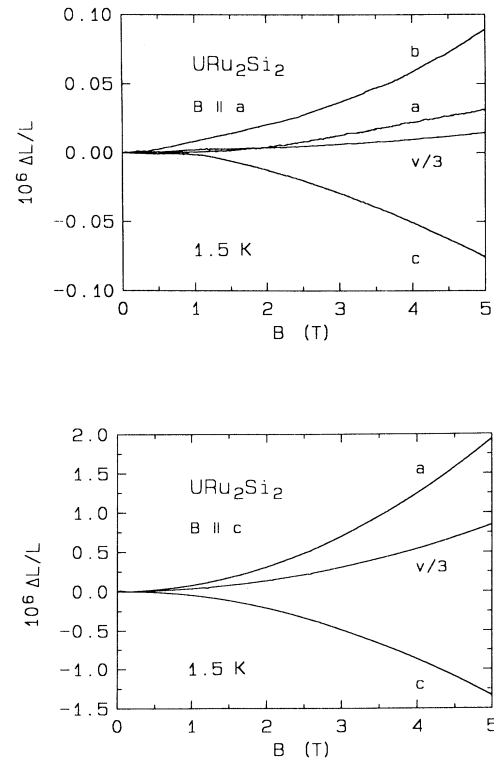


FIG. 5. Normal-state linear magnetostriction of URu₂Si₂ for $\mathbf{B}\parallel a$ and $\mathbf{B}\parallel c$ at 1.5 K. The calculated volume magnetostriction divided by 3 is indicated by $v/3$. Note the different vertical scales for $\mathbf{B}\parallel a$ and $\mathbf{B}\parallel c$.

TABLE I. Quadratic field coefficient b of the magnetostriction $\lambda = bB^2$ for $\Delta L \parallel a, b, c$ and $\mathbf{B} \parallel a, c$ at 1.5 K. The volume magnetostriction is determined by $\lambda_v = \lambda_a + \lambda_b + \lambda_c$ for $\mathbf{B} \parallel a$ and $\lambda_v = 2\lambda_a + \lambda_c$ for $\mathbf{B} \parallel c$.

	$\mathbf{B} \parallel a$	$\mathbf{B} \parallel c$
b_a (10^{-8} T^{-2})	0.13	7.8
b_b (10^{-8} T^{-2})	0.32	
b_c (10^{-8} T^{-2})	-0.31	-5.4
b_v (10^{-8} T^{-2})	0.13	10.2

the linear magnetostriction shows a pronounced hysteresis. The hysteresis loop closes at B_{c2} . For $B > B_{c2}$ the usual B^2 behavior is observed. Remarkably, at the lowest temperatures, in the superconducting state, the hysteresis changes sign at a field close to B_{c2} . With increasing temperature, the inversion point of the hysteresis moves to lower field values, and, finally, vanishes for a temperature close to 1.0 K. Data for λ_a and λ_c ($\mathbf{B} \parallel c$) obtained by the discrete method at $T=0.5$ K are shown in Fig. 7. In Fig. 7, a $\lambda = bB^2$ term, representing the normal-state contribution determined in the field range $B > B_{c2}$ (≈ 2 T), is subtracted. The results of the discrete and sweep methods are in good agreement. Note that in low fields the hysteresis in λ_a has a different sign compared to the hysteresis in λ_c . The aforementioned inversion of the hysteresis close to B_{c2} for λ_c is not observed for λ_a . However, the hysteresis in λ_a becomes negligibly small in that field region. The complex behavior of the magnetostriction is furthermore illustrated by a sign reversal of the hysteresis loop in λ_a by raising the temperature to 1.0 K.

The linear magnetostriction in the superconducting state for a field direction in the tetragonal plane ($\mathbf{B} \parallel a$) at $T=1.0$ K is shown in Fig. 8, with the normal-state background subtracted. The distortions in the basal plane are nearly isotropic. The size of the hysteresis is much small-

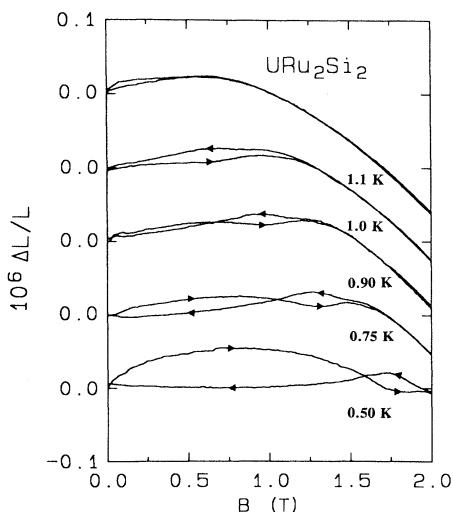


FIG. 6. Sweep measurements of the linear magnetostriction λ_c at $T=0.50, 0.75, 0.90, 1.0,$ and 1.1 K for $\mathbf{B} \parallel c$. The magnetostriction curves are shifted along the vertical axis for sake of clarity.

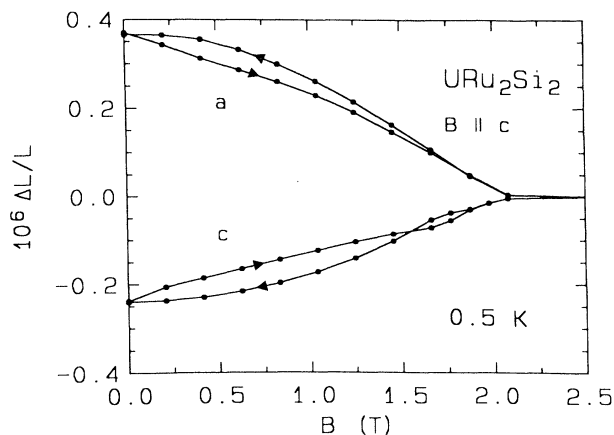


FIG. 7. Discrete measurement of the linear magnetostriction λ_a and λ_c in the superconducting state ($T=0.5$ K) for $\mathbf{B} \parallel c$. The quadratic field dependence of the normal state is subtracted. The magnetostrictive hysteresis for λ_c in the superconducting state changes sign close to the upper critical field where the hysteresis loop closes. The full curves are guides to the eye.

er than observed for $\mathbf{B} \parallel c$. The hysteresis in the λ_b curve seems to show a sign reversal near 1.5 T ($\mathbf{B} \parallel a$). However, the size of the hysteresis for $B > 1.5$ T is of the order of the experimental accuracy.

IV. DISCUSSION AND ANALYSIS

A. Grüneisen parameters

In order to study the volume dependence of the thermal and magnetic energy scales of the heavy-fermion state a Grüneisen parameter analysis is performed.¹⁸ The

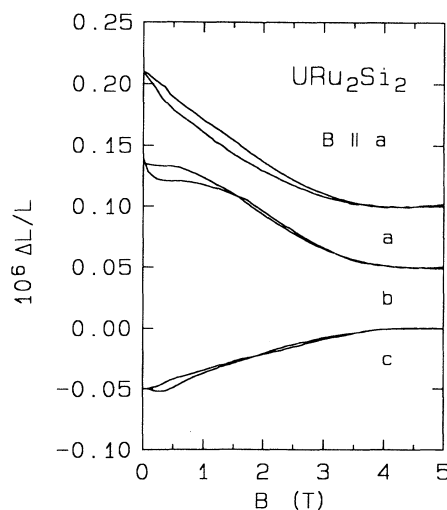


FIG. 8. Sweep measurements of the linear magnetostriction $\lambda_a, \lambda_b,$ and λ_c at $T=1.0$ K for $\mathbf{B} \parallel a$. The quadratic field dependence of the normal state is subtracted. Note that the curves of λ_a and λ_b are shifted along the vertical axis for the sake of clarity.

thermal Grüneisen parameter is defined as $\Gamma_T = -d \ln T^*/d \ln V$, where T^* is the characteristic temperature of the heavy-fermion resonance. The corresponding magnetic Grüneisen parameter is defined as $\Gamma_B = -d \ln B^*/d \ln V$, where B^* is the characteristic field for the heavy-fermion state. One can introduce an experimental effective thermal Grüneisen parameter $\Gamma_{\text{eff}}(T)$ defined by

$$\Gamma_{\text{eff}}(T) = \frac{V_m \alpha_v(T)}{\kappa c(T)}, \quad (1)$$

where $V_m = 4.9 \times 10^{-5} \text{ m}^3/\text{mol}$ is the molar volume and c is the molar specific heat at constant volume. The isothermal compressibility, $\kappa = -V^{-1}dV/dp$, is estimated at 0.73 Mbar^{-1} .¹⁹ In general, it is observed that $\Gamma_{\text{eff}}(T)$ increases rapidly with decreasing temperature as the heavy-fermion state stabilizes. In the low-temperature limit, Γ_{eff} attains a constant value as only the linear terms in the thermal expansion ($\alpha_v = a_v T$) and the specific heat ($c = \gamma T$) are retained and thus $\Gamma_{\text{eff}} = \Gamma_T$, where

$$\Gamma_T = \frac{V_m a_v}{\kappa \gamma}. \quad (2)$$

In the case of URu_2Si_2 , we obtain $\Gamma_T = 27 \pm 2$, where we used $a_v = 0.27 \times 10^{-6} \text{ K}^{-2}$ and $\gamma = 67 \text{ mJ/mol K}^2$. When superconductivity sets in, the effective Grüneisen parameter changes sign and takes the value $\Gamma_{\text{eff}} = -27 \pm 3$. The normal-state thermal Grüneisen parameter can be rewritten as $\Gamma_T = d \ln \gamma / d \ln V$ since $T^* \propto 1/\gamma$. The large value for Γ_T yields a strong suppression of the γ value with pressure: $d \ln \gamma / dp = -\kappa \Gamma_T = -20 \pm 2 \text{ Mbar}^{-1}$. This is in agreement with specific-heat measurements under pressure performed on a polycrystalline sample yielding $d \ln \gamma / dp = -28 \text{ Mbar}^{-1}$.²⁰

The normal-state coefficient of the volume magnetostriiction, $\tau_v = V^{-1}dV/dB$, can be related to the hydrostatic pressure dependence of the magnetization by one of the Maxwell relations:

$$\left[\frac{\partial M}{\partial p} \right]_{B,T} = - \left[\frac{\partial V}{\partial B} \right]_{p,T}. \quad (3)$$

For a quadratic field dependence of the volume magnetostriiction, $\lambda_v = b_v B^2$, a linear field dependence, $\tau_v = 2b_v B$, is found. The hydrostatic-pressure dependence of the molar susceptibility $\chi = \mu_0 M / B$ can be calculated from the relation

$$\left[\frac{\partial \ln \chi}{\partial p} \right]_{B,T} = - \frac{2b_v \mu_0 V_m}{\chi}. \quad (4)$$

The molar susceptibility (in SI units) of URu_2Si_2 at 1.5 K is given by $\chi = 62 \times 10^{-9} \text{ m}^3/\text{mol}$ for $\mathbf{B}||c$ and $\chi = 15 \times 10^{-9} \text{ m}^3/\text{mol}$ for $\mathbf{B}||a$.² Using the coefficients b_v listed in Table I, a value for $d \ln \chi / dp$ of -20 ± 2 and $-1.0 \pm 0.5 \text{ Mbar}^{-1}$ is derived for $\mathbf{B}||c$ and $\mathbf{B}||a$, respectively. Magnetization measurements²¹ under pressures of 1 bar and 4.6 kbar yield a somewhat larger value, $d \ln \chi / dp = -29 \text{ Mbar}^{-1}$ for $\mathbf{B}||c$ at 4.2 K. This suggests that the initial pressure dependence of the susceptibility is apparently smaller than the value at several kbar. The

hydrostatic-pressure dependence of the susceptibility can also be expressed by $-\kappa d \ln \chi / d \ln V$. The corresponding values of $d \ln \chi / d \ln V$ are 25 ± 2 for $\mathbf{B}||c$ and 1.6 ± 0.8 for $\mathbf{B}||a$. The magnetic Grüneisen parameter Γ_B is determined by¹⁸

$$\frac{d \ln \chi}{d \ln V} = (2\Gamma_B - \Gamma_T) + \Gamma_T \frac{d \ln \chi}{d \ln T}, \quad (5)$$

where the last term can be neglected as the susceptibility is temperature independent at low temperatures. The evaluated values of the magnetic Grüneisen parameter at 1.5 K are $\Gamma_B = 26 \pm 3$ ($\mathbf{B}||c$) and $\Gamma_B = 14 \pm 2$ ($\mathbf{B}||a$). For the easy direction of magnetization ($\mathbf{B}||c$) we find $\Gamma_B \approx \Gamma_T$, indicating that the magnetic and thermal properties of the electronic system are strongly coupled in URu_2Si_2 . A similar coupling has been reported for UPt_3 and CeRu_2Si_2 ^{12,22} and appears to be a general feature of heavy-fermion systems. For the hard magnetic axis ($\mathbf{B}||a$) this coupling is absent.

B. Uniaxial pressure dependence of T_c

The uniaxial pressure dependence of the superconducting transition temperature can be determined with one of the Ehrenfest relations for a second-order phase transition:

$$\left[\frac{\partial T_c}{\partial p_i} \right]_{Bp'} = \frac{V_m \Delta \alpha_i}{\Delta(c/T)}, \quad (6)$$

where $i = a, c$ refers to uniaxial pressure along the a or c axis. Values for dT_c / dp_i have been determined from the measured steps in the coefficients of linear thermal expansion, $\Delta \alpha_a$ and $\Delta \alpha_c$, and the step in the coefficient of the linear term in the specific heat, $\Delta(c/T)$, as listed in Table II. We calculate $dT_c / dp_a = -62 \text{ mK/kbar}$ and $dT_c / dp_c = 43 \text{ mK/kbar}$. The hydrostatic-pressure dependence of T_c is given by

$$dT_c / dp = 2dT_c / dp_a + dT_c / dp_c = -81 \text{ mK/kbar}.$$

These values are almost a factor of 2 larger than the ones obtained by resistivity measurements under uniaxial pressure,²³ which yield $dT_c / dp_a = -35 \text{ mK/kbar}$, $dT_c / dp_c = 25 \text{ mK/kbar}$, and $dT_c / dp = -45 \text{ mK/kbar}$. The determination of T_c in these experiments, however, is not

TABLE II. Thermodynamical properties at the superconducting transition $T_c = 1.18 \text{ K}$ in zero field. From the measured steps in the thermal expansion $\Delta \alpha_a, \Delta \alpha_c$ and the specific heat $\Delta(c/T)$, the steps in the compliances Δs_{11} and Δs_{33} and the uniaxial pressure dependence of T_c are determined by the Ehrenfest relations.

$\Delta(c/T)$ (mJ/mol K ²)	54
$\Delta \alpha_a$ (10^{-6} K^{-1})	-0.68
$\Delta \alpha_c$ (10^{-6} K^{-1})	0.47
Δs_{11} ($10^{-6} \text{ Mbar}^{-1}$)	42
Δs_{33} ($10^{-6} \text{ Mbar}^{-1}$)	20
dT_c / dp_a (mK/kbar)	-62
dT_c / dp_c (mK/kbar)	43

unambiguous as the transition broadens under pressure. Better agreement is found with recent specific-heat measurements under uniaxial pressure along the a axis $dT_c/dp_a = -63$ mK/kbar.²⁴ The calculated value for dT_c/dp of -81 mK/kbar may furthermore be compared with the values of -95 and -56 mK/kbar deduced from resistivity²⁵ and specific-heat²⁰ measurements under hydrostatic pressure, respectively. The Grüneisen parameter for the superconducting state,

$$\Gamma_s = -d \ln T_c / d \ln V = \kappa^{-1} d \ln T_c / dp ,$$

amounts to -94 . The anomalies in the compliances Δs_{11} and Δs_{33} are determined by rewriting the Ehrenfest relation [Eq. (6)] in the following form:

$$\left(\frac{\partial T_c}{\partial p_i} \right)_{Bp'} = \frac{\Delta s_{ii}}{\Delta \alpha_i} . \quad (7)$$

The calculated anomalies in the compliances are also listed in Table II. The corresponding steps in the elastic constants at T_c have been determined by sound-velocity measurements.²⁶ Unfortunately, a comparison of the measured anomalies in the elastic constants and the calculated compliances is not possible because not all the relevant elastic constants are known.

C. Magnetostriction in the superconducting state

The condensation energy of the superconducting state, expressed by the energy difference (per unit volume) between the Meissner state and the normal state, is described by $B_c^2/2\mu_0$, where B_c is the thermodynamical critical field. The spontaneous magnetostriction of the superconducting state, $\Delta_{N-S}\lambda_v = (V_S - V_N)/V_N$, is determined by the pressure dependence of the condensation energy:²⁷

$$\Delta_{N-S}\lambda_v = \kappa \frac{B_c^2}{2\mu_0} - \frac{B_c}{\mu_0} \left(\frac{\partial B_c}{\partial p} \right) . \quad (8)$$

The relative length change due to the pressure dependence of the condensation energy, $\Delta_{N-S}\lambda_i = (L_S - L_N)/L_N$, is found by integrating the difference between the measured coefficient of thermal expansion in the superconducting (α_i^S) and the extrapolated normal-state behavior ($\alpha_i^N = a_i T$, where a_i is deduced for $T > T_c$):

$$\Delta_{N-S}\lambda_i = \int (\alpha_i^S - \alpha_i^N) dT . \quad (9)$$

In Fig. 9, λ_a and λ_c are shown as function of T^2 . Above T_c , λ_a and λ_c are quadratic in temperature. At T_c , a change of slope is observed. Below T_c , the spontaneous magnetostriction appears. The relative volume change is $\Delta_{N-S}\lambda_v = 0.48 \times 10^{-6}$ at 0.5 K and $\Delta_{N-S}\lambda_v = 0.17 \times 10^{-6}$ at 1.0 K.

The spontaneous magnetostriction can also be estimated by subtracting a bB^2 term, representing the normal-state magnetostriction (where b is determined by the magnetostriction measured for $B > B_{c2}$), from the magnetostriction in the superconducting state. The relative length change at $B=0$ T then corresponds to the spontaneous magnetostriction. The spontaneous magneto-

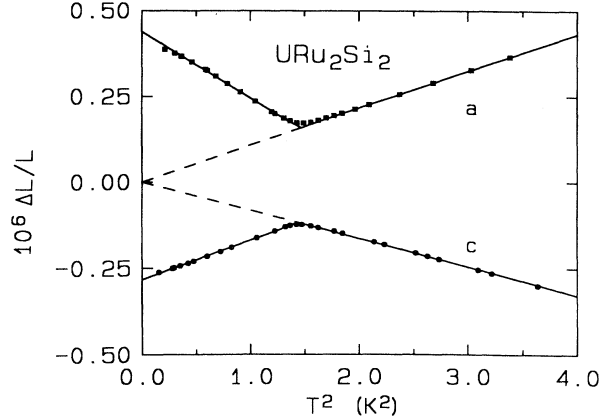


FIG. 9. Relative length change as function of the temperature squared as determined by integration of the linear thermal expansion. At $T_c = 1.18$ K a kink in the relative length is observed. The dashed line represents an extrapolation of the normal-state behavior below T_c . The difference between the extrapolated relative length of the normal state and the relative length of the superconducting state corresponds to the spontaneous magnetostriction.

striction deduced in this manner is shown in Fig. 7 for $\mathbf{B} \parallel c$ (at 0.5 K) and in Fig. 8 for $\mathbf{B} \parallel a$ (at 1.0 K). The values for the spontaneous magnetostriction as evaluated from the magnetostriction are listed in Table III. A good agreement is observed with the values evaluated from the thermal expansion.

The thermodynamical critical field B_c can be estimated from the jump in the specific heat at the superconducting transition in zero field:

$$\Delta(c/T) = \frac{V_m}{\mu_0} \left[\frac{\partial B_c}{\partial T} \right]^2 . \quad (10)$$

From the data in Table II, we calculate $dB_c/dT = -37$ mT/K. The volume change ($\Delta_{N-S}\lambda_v$) caused by the first term in Eq. (8) equals 4×10^{-9} at 0.5 K and 3×10^{-10} at 1.0 K. As the contribution of this first term is negligible with respect to the measured values, which are three orders of magnitude larger, the spontaneous magnetostriction is predominantly attributed to the pressure dependence of B_c . The estimated pressure dependence of B_c , as determined from the second term of Eq. (8), is equal to $dB_c/dp = -2.4$ mT/kbar at 0.5 K. The corresponding uniaxial pressure dependence of B_c is given by $dB_c/dp_a = -1.8$ mT/kbar and $dB_c/dp_c = 1.2$ mT/kbar.

TABLE III. Relative length change $\Delta_{N-S}\lambda$ related to the condensation energy of the superconducting state for $\mathbf{B} \parallel a, c$.

	$\mathbf{B} \parallel a$ ($T=1.0$ K)	$\mathbf{B} \parallel c$ ($T=0.5$ K)
$\Delta_{N-S}\lambda_a$ (10^{-6})	0.11	0.37
$\Delta_{N-S}\lambda_b$ (10^{-6})	0.09	
$\Delta_{N-S}\lambda_c$ (10^{-6})	-0.05	-0.24
$\Delta_{N-S}\lambda_v$ (10^{-6})	0.15	0.50

An effective Ginzburg-Landau parameter κ_{GL} can be introduced by $B_{c2} = \sqrt{2\kappa_{\text{GL}}} B_c$. This effective κ_{GL} can be expressed in anisotropic Ginzburg-Landau parameters by $\kappa_{\text{GL}} = (\kappa_{\text{GL}}^a \kappa_{\text{GL}}^c)^{1/2}$ for $\mathbf{B} \parallel a$ and $\kappa_{\text{GL}} = \kappa_{\text{GL}}^a$ for $\mathbf{B} \parallel c$. Dilatation experiments at 1 K indicate a slope of the upper critical field of -6.25 T/K for $\mathbf{B} \parallel c$ and -19.4 T/K for $\mathbf{B} \parallel a$, in reasonable agreement with previous measurements.^{8,28} Using the measured slopes of B_{c2} and the calculated slope of B_c , the following values for the Ginzburg-Landau parameters are found: $\kappa_{\text{GL}}^a = 119$ and $\kappa_{\text{GL}}^c = 1155$. The lower critical field B_{c1} is of the order of $B_c \ln(\kappa_{\text{GL}}) / \sqrt{2\kappa_{\text{GL}}}$ and therefore negligibly small in our magnetostriction experiments.

The diamagnetic shielding of an external field in the superconducting state is reflected by the forced magnetostriction. The forced magnetostriction in the superconducting state of URu₂Si₂ is found to depend on the history with respect to the external field, i.e., on the hysteresis in the magnetostriction for increasing and decreasing fields. The most obvious origin of this hysteresis is flux-pinning effects, which lead to different flux profiles for increasing and decreasing fields in the sample. The local stress associated with the field penetration is²⁹

$$\sigma(x) = -\frac{B_e^2 - B(x)^2}{2\mu_0}, \quad (11)$$

where B_e is the external field and $B(x)$ is the local field in the sample. The local stress is oriented perpendicular to the external field and points inwards for increasing and outwards for decreasing fields. For fields along the c axis, the local strains along and perpendicular to the field are $\epsilon_{\parallel}(x) = s_{13}\sigma(x)$ and $\epsilon_{\perp}(x) = s_{11}\sigma(x)$, where s_{11} and s_{13} are the compliances. The total linear magnetostriction is found by integrating the local strain over the size of the sample. For a magnetostriction perpendicular to the direction of the field, the length of the sample is smaller for increasing fields than for decreasing fields due to the flux-pinning effects. For a magnetostriction along the field the hysteresis has opposite sign as the compliance s_{13} is negative and s_{11} is positive.

The measured magnetostriction of URu₂Si₂ is not fully consistent with the simple picture described above as a change of sign is observed in the hysteresis. In the low-field and low-temperature range, the appropriate sign for the discussed flux-pinning effects is found, while in the region close to B_{c2} an opposite sign for the hysteresis is observed.

Due to the flux pinning the flux profile inside the sample is different for increasing and decreasing fields in the superconducting state. The hysteresis in the flux profile can be accompanied by hysteresis in both the paramagnetic magnetostriction and the ordered moment. Neutron-diffraction measurements³⁰ for $\mathbf{B} \parallel c$ indeed show a distinct difference between the zero-field-cooled and the field-cooled value of the ordered moment, which is absent in the normal state ($B > B_{c2}$). The observed hysteresis in the ordered moment is of the order of 2%. The contribution of the hysteresis in the ordered moment to the magnetostriction is expected to be relatively small as the normal-state magnetostriction is dominated by the

paramagnetic contribution.

If a similar hysteresis, as observed for the ordered moment, is assumed for the paramagnetic contribution in the superconducting state then the hysteresis of the paramagnetic contribution can be determined from the normal-state magnetostriction (Fig. 5). A hysteresis of 2% in the paramagnetic contribution corresponds to a magnetostrictive hysteresis of 5×10^{-9} for a field of the order of the upper critical field. The sign of this contribution is in agreement with the observed magnetostrictive hysteresis close to B_{c2} in the superconducting state (Fig. 6). The size of the magnetostrictive hysteresis close to the upper critical field is somewhat larger but of the same order of magnitude. Therefore a competition between the superconducting and paramagnetic hysteresis, caused by flux pinning, may account for the observed magnetostrictive hysteresis. Further, we mention that a weak ferromagnetic instability has been reported at 35 K for some of the URu₂Si₂ samples.³¹ The possible presence of a weak ferromagnetic instability has not been examined for our sample. However, because of the absence of any signature of the ferromagnetic order in the normal-state magnetostriction in the form of deviations from the paramagnetic behavior or hysteresis, we do not expect it to be significant for the magnetostrictive hysteresis in the superconducting state.

It is interesting to note that the magnetostriction of the heavy-fermion superconductor UPt₃ shows no significant hysteresis,³² while the magnetostriction of UBe₁₃ exhibits a large hysteresis for dilatations along the magnetic field.³³ The observed hysteresis in the magnetostriction of UBe₁₃ shows the same sign as observed in the region close to the upper critical field in URu₂Si₂, while no long-range magnetic order has been reported for UBe₁₃.

V. CONCLUSIONS

Detailed thermal-expansion and magnetostriction measurements were performed both in the normal state and in the superconducting state of URu₂Si₂ in fields up to 5 T for all relevant crystallographic orientations. Thermal-expansion measurements confirm the presence of an inversion of the linear thermal expansion for all orientations at $T_c = 1.18$ K.

A Grüneisen parameter analysis shows that the thermal and magnetic properties of the electronic system are closely coupled as $\Gamma_T = 27$ and $\Gamma_B = 26$. The steps in the thermodynamical properties at the superconducting transition are analyzed in terms of the Ehrenfest relations. In zero field, the uniaxial pressure dependence of T_c is derived: $dT_c/p_a = -62$ mK/kbar and $dT_c/p_c = 43$ mK/kbar.

The spontaneous magnetostriction, related to the pressure dependence of the condensation energy of the superconducting state, is determined from measurements of the relative length change as a function of field and temperature. The observed spontaneous magnetostriction reflects the strong pressure dependence of the thermodynamical critical field. Magnetostriction measurements reveal hysteresis with an unusual change of sign close to the upper critical field. The unusual change of sign in the

magnetostrictive hysteresis is accompanied by hysteresis in the antiferromagnetically ordered moment in the superconducting state, and possibly reflects the hysteresis in the paramagnetic magnetostriction of superconducting URu_2Si_2 .

ACKNOWLEDGMENTS

This work was part of the research programme of the "Stichting FOM" (Dutch Foundation for Fundamental Research of Matter).

- ¹W. Schlabitz, J. Bauman, B. Politt, U. Rauchschwalbe, H. M. Mayer, U. Ahlheim, and C. D. Bredl, *Z. Phys. B* **52**, 171 (1986).
- ²T. T. M. Palstra, A. A. Menovsky, J. van den Berg, A. J. Dirkmaat, P. H. Kes, G. J. Nieuwenhuys, and J. A. Mydosh, *Phys. Rev. Lett.* **55**, 2727 (1986).
- ³M. B. Maple, J. W. Chen, Y. Dalichaouch, T. Kohara, C. Rossel, M. S. Torikachvili, M. W. McElfresh, and J. W. Thompson, *Phys. Rev. Lett.* **56**, 185 (1986).
- ⁴A. de Visser, F. E. Kayzel, A. A. Menovsky, J. J. M. Franse, J. van der Berg, and G. J. Nieuwenhuys, *Phys. Rev. B* **34**, 8168 (1986).
- ⁵C. Broholm, J. K. Kjems, W. J. L. Buyers, P. Matthews, T. T. M. Palstra, A. A. Menovsky, and J. A. Mydosh, *Phys. Rev. Lett.* **58**, 1467 (1987).
- ⁶M. B. Walker, W. J. L. Buyers, Z. Tun, W. Que, A. A. Menovsky, and J. D. Garrett, *Phys. Rev. Lett.* **71**, 2630 (1993).
- ⁷G. J. Nieuwenhuys, *Phys. Rev. B* **35**, 5260 (1987).
- ⁸J. P. Brison, N. Keller, P. Lejay, A. Huxley, L. Schmidt, A. Buzdin, N. R. Bernhoeft, V. P. Mineev, A. N. Stepanov, J. Flouquet, D. Jaccard, S. R. Julian, and G. G. Lonzarich, *Physica B* **199-200**, 70 (1994).
- ⁹K. Hasselbach, P. Lejay, and J. Flouquet, *Phys. Lett. A* **156**, 313 (1991).
- ¹⁰K. Asyama, Y. Kitaoka, and Y. Kohori, *J. Magn. Magn. Mater.* **76-77**, 449 (1988).
- ¹¹K. Hasselbach, J. R. Kirtley, and P. Lejay, *Phys. Rev. B* **46**, 5826 (1992).
- ¹²A. de Visser, F. E. Kayzel, A. A. Menovsky, J. J. M. Franse, K. Hasselbach, A. Lacerda, L. Taillefer, J. Flouquet, and J. L. Smith, *Physica B* **165-166**, 375 (1990).
- ¹³F. E. Kayzel, A. de Visser, A. A. Menovsky, and J. J. M. Franse, *Physica B* **147**, 231 (1987).
- ¹⁴A. Menovsky and J. J. M. Franse, *J. Cryst. Growth* **65**, 286 (1983).
- ¹⁵A. de Visser, Ph.D. thesis, University of Amsterdam, 1986.
- ¹⁶M. Sigrüst and K. Ueda, *Rev. Mod. Phys.* **63**, 239 (1990).
- ¹⁷E. A. Knetsch, J. J. Peterson, A. A. Menovsky, M. W. Meisel, G. J. Nieuwenhuys, and J. A. Mydosh, *Europhys. Lett.* **19**, 637 (1992).
- ¹⁸P. Thalmeier and P. Fulde, *Europhys. Lett.* **1**, 367 (1986).
- ¹⁹A. de Visser, J. J. M. Franse, and J. J. M. Flouquet, *Physica B* **161**, 324 (1989).
- ²⁰R. A. Fisher, S. Kim, Y. Wu, N. E. Phillips, M. W. McElfresh, M. S. Torikachvili, and M. B. Maple, *Physica B* **163**, 419 (1990).
- ²¹E. Louis, A. de Visser, A. Menovsky, and J. J. M. Franse, *Physica B* **144**, 48 (1986).
- ²²A. B. Kaiser and O. Fulde, *Phys. Rev. B* **37**, 5357 (1988).
- ²³K. Bakker, A. de Visser, A. Brück, A. A. Menovsky, and J. J. M. Franse, *J. Magn. Magn. Mater.* **108**, 63 (1992).
- ²⁴K. Bakker, Ph.D. thesis, University of Amsterdam, 1993.
- ²⁵M. W. McElfresh, J. D. Thompson, J. O. Willis, M. B. Maple, T. Kohara, and M. S. Torikachvili, *Phys. Rev. B* **35**, 43 (1987).
- ²⁶P. Thalmeier, B. Wolf, D. Weber, G. Bruls, B. Lüthi, and A. A. Menovsky, *Physica C* **175**, 61 (1991).
- ²⁷H. Kronmüller, *Phys. Status Solidi* **40**, 295 (1970).
- ²⁸V. V. Moshchalkov, F. Aliev, V. Kovachik, M. Zalyaljutdinov, T. T. M. Palstra, A. A. Menovsky, and J. A. Mydosh, *J. Appl. Phys.* **63**, 3414 (1988).
- ²⁹H. Ikuta, N. Hirota, Y. Nakayama, K. Kishio, and K. Kitazawa, *Phys. Rev. Lett.* **70**, 2166 (1993).
- ³⁰T. E. Mason, H. Lin, M. F. Collins, W. J. L. Buyers, A. A. Menovsky, and J. A. Mydosh, *Physica B* **163**, 45 (1990).
- ³¹A. P. Ramirez, T. Siegrist, T. T. M. Palstra, J. D. Garrett, E. Bruck, A. A. Menovsky, and J. A. Mydosh, *Phys. Rev. B* **44**, 5392 (1991).
- ³²N. H. van Dijk, A. de Visser, J. J. M. Franse, S. Holtmeier, L. Taillefer, and J. Flouquet, *Phys. Rev. B* **48**, 1299 (1993).
- ³³A. de Visser, N. H. van Dijk, J. J. M. Franse, K. Bakker, A. Lacerda, J. Flouquet, Z. Fisk, and J. L. Smith, *Phys. Rev. B* **45**, 2962 (1992).